Inelastic mean free path from reflectivity of slow electrons

R. Zdyb,[1] T. O. Menteş,[2] A. Locatelli,[2] M. A. Niño,[2] and E. Bauer[3]
[1]*Institute of Physics, Maria Curie-Sklodowska University, 20-031 Lublin, Poland*
[2]*Sincrotrone Trieste, S.S. 14 km 163.5, 34149 Basovizza (TS), Italy*
[3]*Department of Physics, Arizona State University, Tempe, Arizona 85287-1504, USA*
(Received 27 November 2012; revised manuscript received 29 January 2013; published 25 February 2013)

The inelastic mean free path (IMFP) of electrons is derived using a new approach based on the low-energy electron reflectivity from ultrathin films. The thickness-dependent quantum size oscillations as a function of electron energy observed in the reflectivity of slow electrons are modeled using an absorbing Fabry-Pérot interferometer consisting of vacuum, film, and substrate. The absorbing properties of the film are represented by the imaginary part of the complex refractive index associated with the IMFP which determines the amplitude of the electron reflectivity oscillations. Using this formalism for an Fe film on W(110), the IMFP in Fe is found in the energy range from 4 to 18 eV above the vacuum level. In contrast to the common notion, the IMFP in Fe is shown to have a very weak energy dependence at low energy. The results are in good agreement with independent IMFP measurements found in thickness-dependent photoemission experiments.

DOI: 10.1103/PhysRevB.87.075436 PACS number(s): 71.20.Be, 73.21.Fg, 73.50.Gr, 75.50.Bb

I. INTRODUCTION

The electron inelastic mean free path (IMFP) plays an important role in the analysis of data obtained by many experimental techniques involving electrons above the vacuum level. At energies above 50 eV methods for the determination of the IMFP are well established and the IMFPs values are well known.[1] In recent years the advance of surface-sensitive techniques has necessitated the knowledge of IMFP also in the energy range below 50 eV.

There are several methods currently used for the determination of the IMFP. In the well-known procedure proposed by Powell, the IMFP is calculated from experimental optical data using the Penn algorithm[2] or measured by elastic peak electron spectroscopy.[1] However, below 50 eV the Penn algorithm does not give reliable results.[3] One other method is based on the measurements of the attenuation of the intensity of electron beam traveling through an absorbing medium. The exponential decay of the photoemission signal from a buried layer as a function of increasing overlayer thickness gives a direct measure of the IMFP (neglecting elastic scattering) in the overlayer material. Recently another approach has been proposed in which high-accuracy measurements of the x-ray absorption fine structure were used.[4] It has been found that the amplitude of oscillations following an absorption edge is strongly influenced by the IMFP. The IMFP is obtained by comparing the theoretical x-ray absorption fine structure spectrum with experimental data. This technique works below 100 eV but not at the very low energies of interest here.

Here, we propose another method for the determination of the IMFP for energies in the range of several eV above the vacuum level. The idea stems from the influence of the IMFP on the amplitude of quantum size oscillations in the low-energy electron reflectivity in ultrathin films. This approach is based on the Fabry-Pérot interferometer model of an absorbing medium and takes into account the band structure of the film. In the following we will describe our model and apply it to experimental low-energy electron reflectivity data from ultrathin Fe films on W(110). As an independent measure of the IMFP at low energies, similar films of Fe/W(110) are used to determine the thickness-dependent attenuation of tungsten core-level photoelectrons.

II. MODEL

The starting point of the model is the expression for the complex reflection coefficient r of light at normal incidence on a thin absorbing film:[5]

$$r = \frac{\rho_{12} + \rho_{23}\, e^{-2\nu_2\eta}\, e^{i2u_2\eta}}{1 + \rho_{12}\rho_{23}\, e^{-2\nu_2\eta}\, e^{i2u_2\eta}}, \tag{1}$$

where the indices 1, 2, and 3 denote the vacuum, the absorbing medium, and the substrate, respectively. $\rho_{12(23)} = |\rho_{12(23)}|e^{i\varphi_{12(23)}}$ is the amplitude of the reflected wave at the specified interface. $u_{2(3)}$ and $\nu_{2(3)}$ are the real and imaginary parts of the complex refractive index of the absorbing medium (substrate), respectively; $\eta = 2\pi h/\lambda_1$, where λ_1 is the wavelength of light in vacuum and h is the thickness of the absorbing medium. The amplitudes of the reflected waves can be derived from the refractive indices as follows:[5]

$$\rho_{12} = \frac{1 - (u_2 + i\nu_2)}{1 + (u_2 + i\nu_2)}, \quad \rho_{23} = \frac{(u_2 + i\nu_2) - (u_3 + i\nu_3)}{(u_2 + i\nu_2) + (u_3 + i\nu_3)}. \tag{2}$$

The energy density decreases to $1/e$ of its initial value after the wave has traveled a distance of $L = 1/\alpha$, where $\alpha = 4\pi\nu_2/\lambda_2$ is the absorption coefficient and λ_2 is the wavelength of light in the absorbing medium.[5] The real parts of the refractive indices of film and substrate are defined as $u_2 = k_2/k_1$ and $u_3 = k_3/k_2$, respectively, where $k_{1,2,3} = 2\pi/\lambda_{1,2,3}$ are the wave vectors in the respective media. Finally, multiplying r by its complex conjugate the reflectivity R is obtained, the quantity which is measured in the experiment. Considering the electron as a wave we define IMFP as the distance L. Together with the energy dependence of the wave vector in the absorbing film $k_2(E)$ and in the substrate $k_3(E)$ the IMFP can be directly incorporated into the model in analogy to the absorption of light.

In order to apply the model to ultrathin Fe films on W(110) to find the Fe IMFP, we need to determine the IMFP in the W(110) substrate, along with the energy-dependent wave

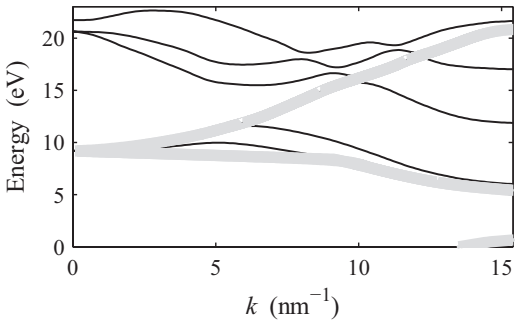

FIG. 1. Tungsten band structure along the [110] direction above the vacuum level. For details see text.

vectors k_2 and k_3. The tungsten IMFP has been calculated according to the expression[6] $L_3 = \sqrt{E}/(a(E+\phi)^b)$ where the values of the coefficients a and b of the imaginary part of the inner potential have been taken from Ref. 7 and the tungsten work function is $\phi = 5.35$ eV. The obtained IMFP values are between 2.7 and 3.0 Å in the considered energy range.

The $k_3(E)$ dependence for the W(110) substrate has been taken from Ref. 13 choosing the bands as proposed by Flege *et al.*[14] In the energy range where there are several bands those which are close to free-electron-like have been chosen; i.e., the electron transmission is affected by a single bulk band with almost parabolic dispersion. The band structure taken from Ref. 13 together with the bands used in our calculations (thick shaded) are shown in Fig. 1.

The $k_2(E)$ dependence has been extracted from the experimental quantum size oscillations in low-energy electron reflectivity.

III. EXPERIMENTAL

Measurements of the reflectivity of slow electrons from ultrathin Fe films on W(110) were carried out in a low-energy electron microscope (LEEM)[9] under ultrahigh vacuum conditions with a base pressure in the low 10^{-10} mbar range. Prior to the Fe deposition the W(110) crystal was cleaned in the standard way by heating in oxygen at 1400 K and then flashing off the remaining oxide layer at 2000 K. The surface quality was checked with low-energy electron diffraction (LEED) and by the step flow growth of Fe at elevated temperature. The Fe islands of different heights were produced by deposition of Fe on the bare W(110) substrate at 550 K. The Fe layer thickness was controlled by the time needed to complete the first pseudomorphic monolayer which gives strong contrast change in the LEEM image and by the quantum size effect (QSE).[8,10]

IV. RESULTS AND DISCUSSION

The results of the reflectivity experiment are shown in Fig. 2(a) for 5, 6, and 7 ML Fe. The experimental data have been normalized to the intensity of the electron beam measured in the mirror microscopy mode.[8] Between the very steep initial reflectivity decrease and the Bragg peak located at above 20 eV, very clear intensity oscillations are visible. In order to determine the band structure of Fe above the

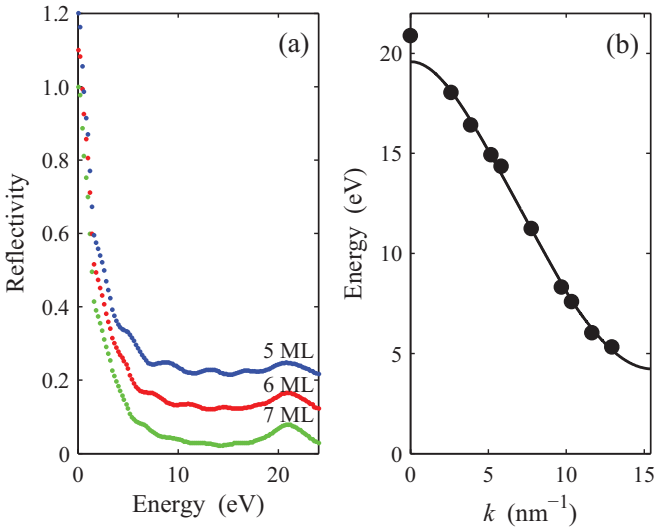

FIG. 2. (Color online) (a) Reflectivity vs energy measured in LEEM. (b) Fe band structure along the [110] direction above the vacuum level derived from LEEM (circles). The solid line is a two-band model fit to the experimental data. Zero denotes the vacuum level.

vacuum level a phase accumulation model has been used,[8] which takes into account the energy positions of the quantum size oscillations shown in Fig. 2(a). The results are shown in Fig. 2(b) (circles) together with the results of a two-band model fit (solid line).[11,12]

The magnitude of the quantum size oscillations in Fig. 2(a) depends sensitively on the Fe IMFP. Figure 3(a) shows experimental (dots) and calculated (solid and dashed lines) reflectivity curves of a 6 ML thick Fe film. The calculations for $L = 5$ Å (solid red) and $L = 7$ Å (dashed blue) show the dramatic effect of the IMFP on the oscillation amplitude. The calculated reflectivity curve is shifted down with respect to the experimental data. The reason for this disagreement is apparently due to the background in the experimental data caused by secondary electrons, inelastic scattering, and other sources. In order to eliminate this background the energy-dependent zero line around which the intensity oscillates has been subtracted. It is obtained by measuring the reflectivity from a thick layer which shows no oscillations because $L \ll h$.[8] The difference curves are displayed in Fig. 3(b).

There are three characteristic features visible in Figs. 3(a) and 3(b). First, the similar oscillatory behavior of both experimental and calculated curves between about 4 and 20 eV shows that the presented model works well in the energy range of the Fe *s-p* band. Below about 4 eV and above 20 eV there are discrepancies between the two curves which are associated with the band gaps in Fe in the [110] direction. This is to be expected because the model used was developed for electromagnetic waves, i.e., for waves without energy gaps. Second, the oscillation amplitude depends very strongly on the value of the IMFP of Fe. Third, there is a small but noticeable energy shift in the position of the peaks which slightly increases with energy. We have made an attempt to correct this shift by introducing an additional fitting term to the phase φ_{12} and obtained the energy-dependent expression

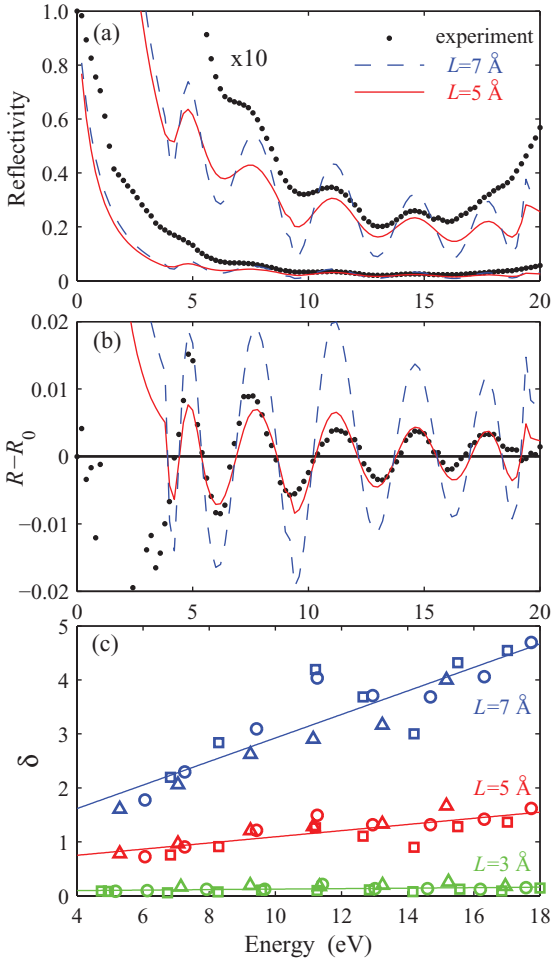

FIG. 3. (Color online) (a) Reflectivity vs energy for 6 ML Fe derived from experiment (dots) and theory (lines) according to Eq. (1). (b) Difference between reflectivity and zero line. For details see text. The line codes in (b) are the same as in (a). (c) Ratio of calculated oscillations amplitude, assuming energy-independent IMFP, to amplitude determined from experiment. Triangles, circles, and squares are from 5, 6, and 7 ML data, respectively. Zero denotes the vacuum level.

for the phase $\varphi_{12}^{\mathrm{corr}} = \varphi_{12} - 0.0035E^2 + 0.1E$, where E is the electron energy. This improves the agreement between the calculated and experimental data mainly in the higher energy range, Fig. 3(b). It is interesting to note that a similar shift was found in 5 and 7 ML thick films and that the same correction formula works also for them. This suggests the same mechanism responsible for the observed shift. It might be due to adsorption of residual gases during the several hours lasting experiments which can influence the phase at the film/vacuum interface. The shift does not change the oscillation amplitude; therefore it does not influence the value of the IMFP. Figure 3(c) shows the ratio of the oscillation amplitudes calculated for $L = 3$ Å (green), 5 Å (red), and 7 Å (blue) to the amplitude determined in the experiment. Triangles, circles, and squares are from 5, 6, and 7 ML data, respectively. It shows the high sensitivity of the model to the value of the IMFP. Lower or higher values than 5 Å do not fit the data. Moreover, neither is a constant IMFP sufficient to

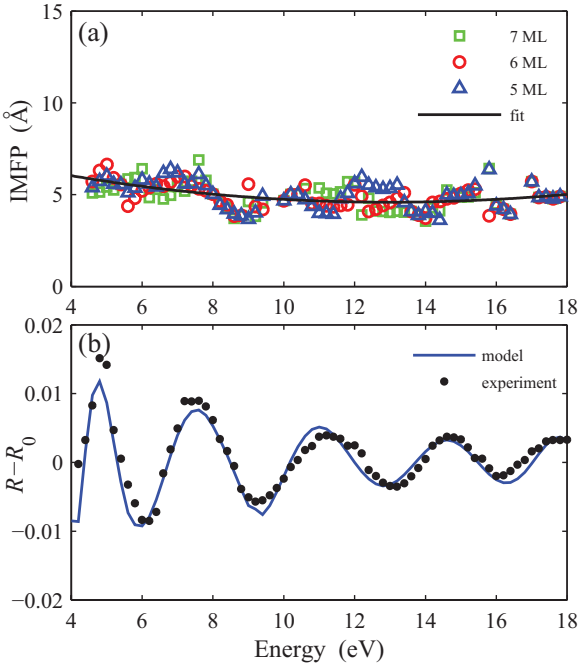

FIG. 4. (Color online) (a) Inelastic mean free path vs energy calculated from Fe reflectivity curves. The black full line is a fit to the mean values. (b) Reflectivity vs energy for 6 ML Fe derived from the experiment (dots) and the model (solid) with L values derived from the fit in (a).

reproduce the experimental data: At low energy the ratio is too small, at high energy too large.

The energy dependence of the IMFP determined from the model analysis (including the phase correction) of the reflectivity curves of 5, 6, and 7 ML thick Fe films is shown in Fig. 4(a). All three sets of results show the same energy dependence. The source of the scatter is the noise in the original reflectivity data. Figure 4(b) shows the experimental reflectivity difference curve (dots) for 6 ML Fe together with the calculated one (solid line) with L values derived from the fit to the average results shown in Fig. 4(a).

In order to have an independent measure of IMFP in Fe, we have carried out photoelectron attenuation measurements in similar Fe/W(110) films using the spectroscopic photoemission low-energy electron microscope (SPELEEM) at the nanospectroscopy beamline (Elettra).[15] The energy-dependent Fe IMFP was extracted from the attenuation of the tungsten $4f$ photoelectrons as a function of Fe thickness with varying photon energy. Spectra from coexisting regions of different thickness were simultaneously measured in a spatially resolved manner in order to avoid potential normalization errors. Due to the small signal level at low energy, the thickest Fe film used was 3 ML. The spectromicroscopy measurements are summarized in the example of Fig. 5. The energy-dependent IMFP results are displayed in Fig. 6 along with the results from the preceding analysis of the quantum size oscillations in electron reflectivity.

There are only a few IMFP data for Fe in the considered energy range in the literature. The results of previously reported spin-resolved IMFP data for Fe[17–19] are of the same order of magnitude as reported here. Pappas *et al.*[17] give the

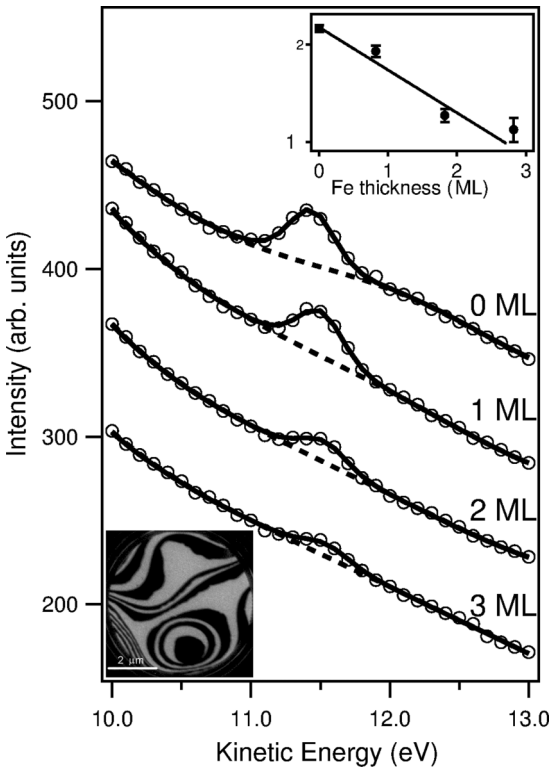

FIG. 5. Example spectra showing the tungsten $4f_{7/2}$ core level as a function of Fe thickness at a photon energy of 46 eV. The bottom inset shows a LEEM image of the submonolayer Fe/W(110) with dark contrast corresponding to the Fe monolayer. The top inset shows the exponential dependence of the W signal vs Fe thickness. The intensity of each peak is found by fitting a Doniach-Šunjić function (Ref. 16) as shown by solid lines along with the data.

attenuation lengths of 5.2, 5.0, and 4.9 Å at energies 4.25, 9.45, and 13.25 eV above the vacuum level, respectively, assuming 4.85 eV for the work function of Fe. The authors report also spin-resolved results: 5.8, 4.7, and 5.0 Å, for spin up, down, and weighted average, respectively, at 7.2 eV. At 14.3 eV the corresponding values are 5.3 and 4.5 Å with a mean value of 4.7 Å. Getzlaff *et al.*[18] report 9.2 and 6.3 Å for spin up and down electrons, respectively, at 9.5 eV, which gives 7.1 Å in weighted average. Passek *et al.*[19] report 11.1 and 6.7 Å for spin up and down electrons, respectively, with weighted average of 8.0 Å at 7.75 eV. The results of Pappas *et al.*[17] agree very well with the results obtained in the reflectivity experiment. The IMFP values reported in Ref. 18,19 are slightly higher than those from the reflectivity experiments, Fig. 6. The obtained results are also in very good agreement with data reported by Paul and coworkers.[20]

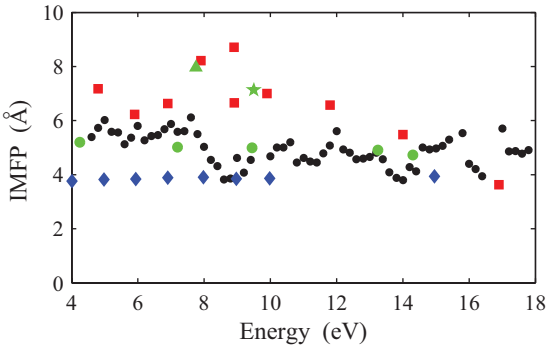

FIG. 6. (Color online) IMFP determined by reflectivity (black dots) and photoemission (red squares) experiments. Green circles, triangle, and star are from Refs. 17–19, respectively, blue diamonds Ref. 24.

These IMFPs of Fe are much smaller than those expected from the "universal curve" in this energy range. They are only about two to three lattice constants while the "universal curve" predicts IMFP of the order of nm.[21] Moreover, the IMFP depends much less on energy than given by the "universal curve" and theoretical calculations.[22,23] However, the observed weak energy dependence is in good agreement with the calculations by Hong and Mills.[24] Although the authors report spin-resolved results the averaged values are about 4 Å in the considered energy range, Fig. 6. This value is very close to our results which are about 5 Å. It is also interesting to notice that a similar energy dependence of the IMFP was recently reported for Cu[4] above about 10 eV. However, below this energy it increases strongly. This shows the limitations of the "universal curve" in the case of the IMFP of Fe at very low energies.

V. SUMMARY

In conclusion we have presented a new approach for the determination of the IMFP in the energy range from 4 to 18 eV. It is based on a Fabry-Pérot interferometer model of an absorbing medium. A comparison of the calculated reflectivity of the interferometer with the measured reflectivity of slow electrons from ultrathin Fe films allows the determination of the IMFP in the absorbing medium. The good agreement between the values of the IMFP in Fe obtained in this manner with the results of other experiments and with calculations confirms the applicability of the presented model.

ACKNOWLEDGMENTS

This work was supported in part by the Polish Ministry of Science and Higher Education under Grant No. N N202 174539.

[1]C. J. Powell and A. Jablonski, J. Phys. Chem. Ref. Data **28**, 19 (1999).
[2]S. Tanuma, C. J. Powell, and D. R. Penn, Surf. Interface Anal. **43**, 689 (2011).
[3]S. Tanuma, C. J. Powell, and D. R. Penn, Surf. Interface Anal. **17**, 911 (1991).
[4]J. D. Bourke and C. T. Chantler, Phys. Rev. Lett. **104**, 206601 (2010).

[5]M. Born and E. Wolf, *Principles of Optics*, 6th ed. (Cambridge University Press, Cambridge, 1980).
[6]B. Ziaja, R. A. London, and J. Hajdu, J. Appl. Phys. **99**, 033514 (2006).
[7]H.-J. Herlt *et al*., Solid State Commun. **38**, 973 (1981).
[8]R. Zdyb and E. Bauer, Phys. Rev. Lett. **88**, 166403 (2002).
[9]E. Bauer, in *Magnetic Microscopy of Nanostructures*, edited by H. Hopster and H. P. Oepen (Springer, Berlin, 2005), p. 111; E. Bauer, in *Modern Techniques for Characterizing Magnetic Materials*, edited by Y. Zhu (Kluwer, Boston, 2005), p. 361.
[10]R. Zdyb and E. Bauer, Surf. Rev. Lett. **9**, 1485 (2002).
[11]S. L. Altmann, *Band Theory of Metals*, 1st ed. (Pergamon Press, 1970).
[12]M. S. Altman, J. Phys.: Condens. Matter **17**, S1305 (2005).
[13]N. E. Christensen and B. Feuerbacher, Phys. Rev. B **10**, 2349 (1974); R. F. Willis and N. E. Christensen, *ibid*. **18**, 5140 (1978).
[14]J. I. Flege, A. Meyer, J. Falta, and E. E. Krasovskii, Phys. Rev. B **84**, 115441 (2011).
[15]A. Locatelli, L. Aballe, T. O. Menteş, M. Kiskinova, and E. Bauer, Surf. Interface Anal. **38**, 1554 (2006).
[16]S. Doniach and M. Šunjić, J. Phys. C **3**, 285 (1970).
[17]D. P. Pappas, K.-P. Kämper, B. P. Miller, H. Hopster, D. E. Fowler, C. R. Brundle, A. C. Luntz, and Z.-X. Shen, Phys. Rev. Lett. **66**, 504 (1991).
[18]M. Getzlaff, J. Bansmann, and G. Schönhense, Solid State Commun. **87**, 467 (1993).
[19]F. Passek, M. Donath, and K. Ertl, J. Magn. Magn. Mater. **159**, 103 (1996).
[20]O. Paul *et al*., Surf. Sci. **251-252**, 27 (1991).
[21]M. P. Seah and W. A. Dench, Surf. Interface Anal. **1**, 2 (1979).
[22]C. J. Tung, J. C. Ashley, and R. H. Ritchie, Surf. Sci. **81**, 427 (1979).
[23]D. R. Penn, Phys. Rev. B **35**, 482 (1987).
[24]J. Hong and D. L. Mills, Phys. Rev. B **62**, 5589 (2000).